JOURNAL OF GEOPHYSICAL RESEARCH, VOL. 99, NO. B6, PAGES 11,575–11,590, JUNE 10, 1994

Lateral variations in D'' thickness from long-period shear wave data

J.-M. Kendall[1] and P. M. Shearer

Institute of Geophysics and Planetary Physics, Scripps Institution of Oceanography, University of California, San Diego, La Jolla

Abstract. We explore global variations in D'' shear wave structure by examining 12 years of long-period Global Digital Seismograph Network (GDSN) data to identify reflected phases from the D'' layer in the lowermost mantle. We restrict our search to epicentral distances between 63° and 74° where a precritical D'' reflection will lie between the S and ScS arrivals. With GDSN long-period records a D'' signal at these ranges is generally obscured by the stronger neighboring phases, so to isolate the D'' reflections we develop a technique for stripping away the interfering S and ScS waveforms. We interpret travel time variations in the observed SdS phases in terms of variations in D'' thickness and generate maps of inferred D'' thickness for areas of good seismic coverage. The regions of observed D'' reflections are beneath Australasia, north central Asia, the Arctic, Alaska, and central America. We find considerable variation in D'' structure in these regions, a result consistent with previous studies which have found evidence for lateral heterogeneity in D''. On average, the estimated D'' thickness is 260 km, but there is a fairly uniform distribution of thicknesses between 150 km and 350 km. A possible correlation is observed between D'' thickness and regions of predicted strong horizontal mantle flow.

Introduction

Global interpretations of an anomalous region at the base of the mantle have been documented in seismological studies as early as those of *Gutenberg* [1914]. *Bullen* [1949] coined the name D'' for the anomalous region of lower mantle located a few hundred kilometers above the core-mantle boundary (CMB). Most globally averaged Earth models predict a D'' region, but its thickness and velocity gradient are quite variable (compare, for example, the Preliminary Reference Earth Model (PREM) [*Dziewonski and Anderson*, 1981] and the Jefferys-Bullen model (JB) [*Jeffreys and Bullen*, 1940]), and a variety of recent studies have suggested that the D'' region has strong lateral variations (see *Lay* [1989] and *Weber* [1993] for references). Much of this work has concentrated on looking for reflections from regional patches of D'' that range widely in size. There had been some evidence for lower mantle discontinuities based on early data sets which were sparse in coverage and low in quality, but it was not until the 1980s that a D'' discontinuity became widely accepted.

Lay and Helmberger [1983] presented the first definitive evidence for such a lower mantle reflector. Since then, Lay and coworkers have continued to use S waveform analysis to study D'' reflections in many regions [*Lay*, 1986; *Young and Lay*, 1987, 1990; *Gaherty and Lay*, 1992]. Other S waveform studies are those of *Weber and Davis* [1990], *Revenaugh and Jordan* [1991], *Weber* [1993], and *Garnero et al.* [1993]. Weber and coworkers have investigated P wave reflections from D'', usually working with high-quality array data (see the studies of *Weber and Davis* [1990], *Weber and Körnig* [1992] (using ISC bulletins), *Weber* [1993], and *Krüger et al.* [1993]. Other P wave studies include those of *Baumgardt* [1989], *Young and Lay* [1989], *Houard and Nataf* [1992], and *Vidale and Benz* [1993]. Cumulatively, this work shows that D'' is a highly variable region that is often a strong reflector of seismic energy. For a summary of regions of identified S and P wave discontinuities, see *Lay* [1989]. More detail of previous work will be given in the results section of this paper. It is important to note that there are also regions where no D'' reflection is observed [*Cormier*, 1985; *Schlittenhardt et al.*, 1985; *Buchbinder*, 1991; *Krüger et al.*, 1993; *Weber*, 1993] and that a D'' discontinuity is not necessarily a global feature.

There are numerous possible explanations for structural heterogeneity at the base of the mantle that in general suggest that D'' is a complicated region that is thermally and chemically distinct from the overlying mantle. D'' may represent a thermal boundary layer

[1]Now at Department of Physics, University of Toronto, Ontario, Canada.

Paper number 94JB00236.
0148-0227/94/94JB-00236$05.00

because of the large temperature differences ($\approx$ 1000°K) between the lower mantle and outer core [*Elasser et al.*, 1979; *Stacey and Loper*, 1983]. It has been postulated that thermal instabilities within this layer could initiate mantle plume formation [*Yuen and Peltier*, 1980; *Stacey and Loper*, 1983]. There is mounting evidence that D'' is also a chemical boundary layer. *Knittle and Jeanloz* [1991] argue, on the basis of high pressure-temperature experiments, that D'' is a reaction zone where lower mantle perovskite interacts with the liquid iron of the outer core. It has also been suggested that subducted lithosphere may accumulate at the base of the mantle [*Silver et al.*, 1988; *Christensen*, 1989], perhaps even in episodic avalanches of subducted material [*Tackley et al.*, 1993]. Furthermore, recent estimates of Poisson's ratio from seismic data also suggest that D'' is chemically distinct from the overlying mantle [*Bolton and Masters*, 1992]. Finally, it has been suggested that a D'' discontinuity may be due to a phase transition, just as upper mantle discontinuities are physical in origin [*Nataf and Houard*, 1993]. Understanding the nature of this major transitional region places important constraints on the dynamics of the Earth as a whole. For example, if D'' serves as a repository for subducted surface material and is the site of mantle plume generation, this will place strong constraints on the style of mantle convection. Mapping global variations in the structure of D'' using seismic data should help resolve these issues.

In an effort to explore such variations in D'' structure we have examined long-period shear wave data from the Global Digital Seismograph Network (GDSN). Seismic energy will be reflected from the top of the D'' layer if there is a velocity discontinuity at this boundary (or a sufficiently steep velocity gradient). Therefore one way of estimating D'' thickness is to search global data sets for these reflections. It is best to look for these phases at large epicentral ranges (i.e., beyond 60°) because reflections from a weak discontinuity like D'' become stronger as the angle of incidence becomes larger. Unfortunately, for long-period data the S and ScS phases interfere with the D'' reflections at these distances. To isolate the D'' reflections, we have developed a technique for stripping away the waveform contributions from the interfering S and ScS phases. Using the phase-stripping technique, we have identified regions where the top of the D'' layer reflects long-period energy. Our results indicate strong lateral variations in D'' thickness.

Phase-Stripping Technique

To help guide our study of long-period SH data, we have generated WKBJ synthetic seismograms [*Chapman*, 1978] for an existing D'' model. Figure 1a shows SH waveforms at epicentral distances ranging from 60° to 80° for the model SGLE of the lower mantle below Eurasia [*Gaherty and Lay*, 1992]. This model has a velocity discontinuity 290 km above the CMB. We have concentrated our search in the 60° to 75° range where

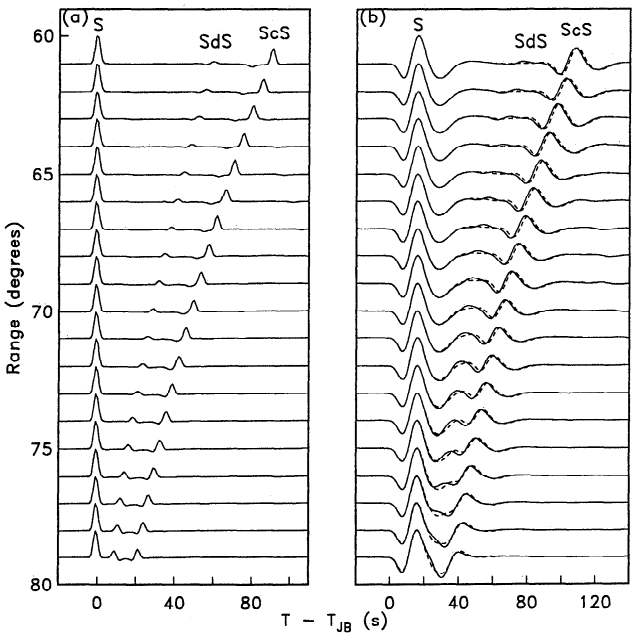

Figure 1. WKBJ SH waveforms for a surface source in the lower mantle model SGLE [*Gaherty and Lay*, 1992] which has a velocity discontinuity 290 km above the core-mantle boundary. Travel times are reduced by the S wave travel times for the *Jeffreys and Bullen* [1940] Earth model. Figure 1a shows the waveforms given a δ-function at a point source. These waveforms are then convolved with the long period SRO instrument response (Figure 1b). The dotted lines show the waveforms for PREM [*Dziewonski and Anderson*, 1981]. Note that SGLE ScS arrivals are slightly earlier than those for PREM due to differences between models in the overall velocity structure within the D'' layer.

the three phases S, ScS, and SdS are simple δ-functions with the same polarity. Following *Weber and Davis* [1990] we use the term SdS for the S phase reflected from D''. Note that a δ-function source pulse is assumed and no instrument response has been included. The SdS amplitudes diminish at closer ranges as they approach a null in the reflection coefficient at 44°; the SdS waveform is reversed in polarity at shorter distances (SH waveforms go through a polarity reversal as the angle of incidence on a discontinuity increases). A simple δ-function waveform is ensured as the SdS phase is precritical in this region and the travel time triplication associated with the D'' discontinuity starts beyond 75°. The reflection from the underside of D'' (henceforth referred to as $SDDS$) is included in these synthetics, but the phase is virtually imperceptible in the region following the ScS phase. This is because of the weakness of the discontinuity and the more vertical incidence angle of this phase in comparison to SdS. In summary, between 60° and 75° only three phases, S, SdS, and ScS, each identical in character and polarity, are visible on the transverse component synthetics within the time window shown.

Figure 1b shows the WKBJ seismograms convolved with a long-period SRO instrument response. The re-

sulting pulse widths make the D'' discontinuity contribution to each seismogram difficult to resolve. Pulse widths in data are likely to be even longer due to attenuation and realistic source-time functions, making it nearly impossible to identify SdS arrivals on individual seismograms. In most previous studies SdS can be distinguished from S and ScS because higher-frequency data were used. The response of the long-period WWSSN data used by Lay and coworkers [e.g., *Lay and Helmberger*, 1983] extends to shorter periods than the GDSN data, a difference which permits direct observations of SdS phases at ranges between about 65° and 80°.

We experimented with stacking techniques on the long-period GDSN data [e.g., *Shearer*, 1991] to see if SdS could be imaged at shorter ranges where it should be separated from ScS. *Revenaugh and Jordan* [1991] reported intermittent observations of a D'' reflector at near-normal incidence angles in GDSN long-period ScS reverberation data. However, our stacks on both S and ScS reference phases were unsuccessful in resolving an SdS phase. This result is not unexpected given the very low amplitudes predicted for SdS phases at ranges less than about 55° (and could also be partially due to large variations in D'' depths). Much higher amplitudes are predicted for SdS above 60° , and it is at these more favorable ranges that almost all observations of D'' reflectors have been made.

In order to examine directly the SdS phase at distance ranges beyond 60° in the long-period GDSN data we have developed a method for removing the S and ScS contributions from the wavetrain. The technique is outlined below and illustrated for synthetic examples in Figures 2 and 3.

Step 1. The S and ScS phases are identified, equivalent peaks are picked, and their waveforms are cross-correlated. Cross-correlation windows surrounding the picks are chosen to be typically one or two cycles in width (dashed segments in Figure 2a). Only seismo-

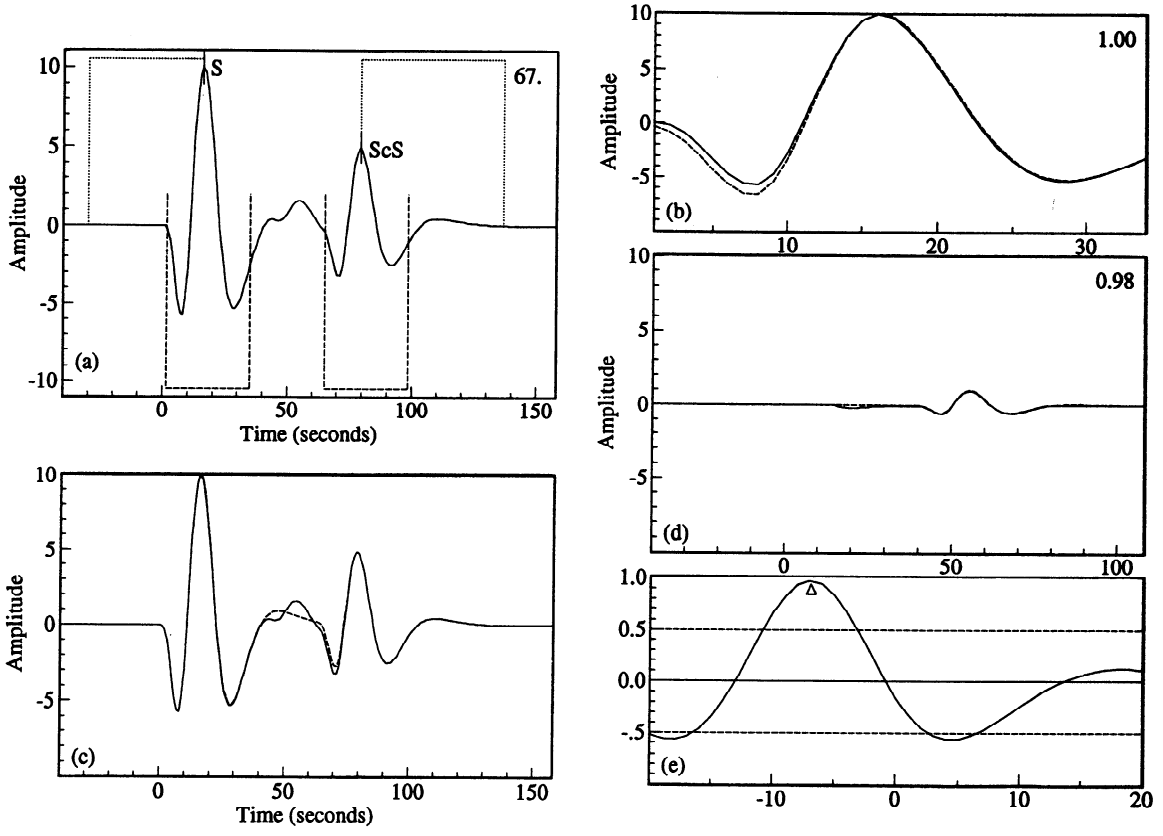

Figure 2. An illustration of the phase-stripping technique applied to the synthetic SH waveform for the model SGLE [*Gaherty and Lay*, 1992] at an epicentral distance of 67°. (a) S and ScS waveforms (dashed lines). The dotted lines show the two constituent parts of the reference pulse which are scaled in amplitude and joined. (b) Correlated S and ScS waveforms. Correlation coefficient is shown in upper right. (c) Original waveform (solid line) and the reference trace (dashed line). The reference trace is formed by the superposition of reference pulses centered and scaled on the picked S and ScS arrivals. (d) Result after the reference trace is subtracted from the original waveform. The resultant SdS waveform is cross-correlated with the reference pulse, and the dashed line is the reference pulse positioned where the cross correlation is best (coefficient is shown in upper right of Figure 2d). (e) Cross-correlation function for the reference pulse and the resultant waveform. The time window is 20 s either side of midway between the S and ScS picks. The triangle indicates the time shift which optimizes the cross correlation.

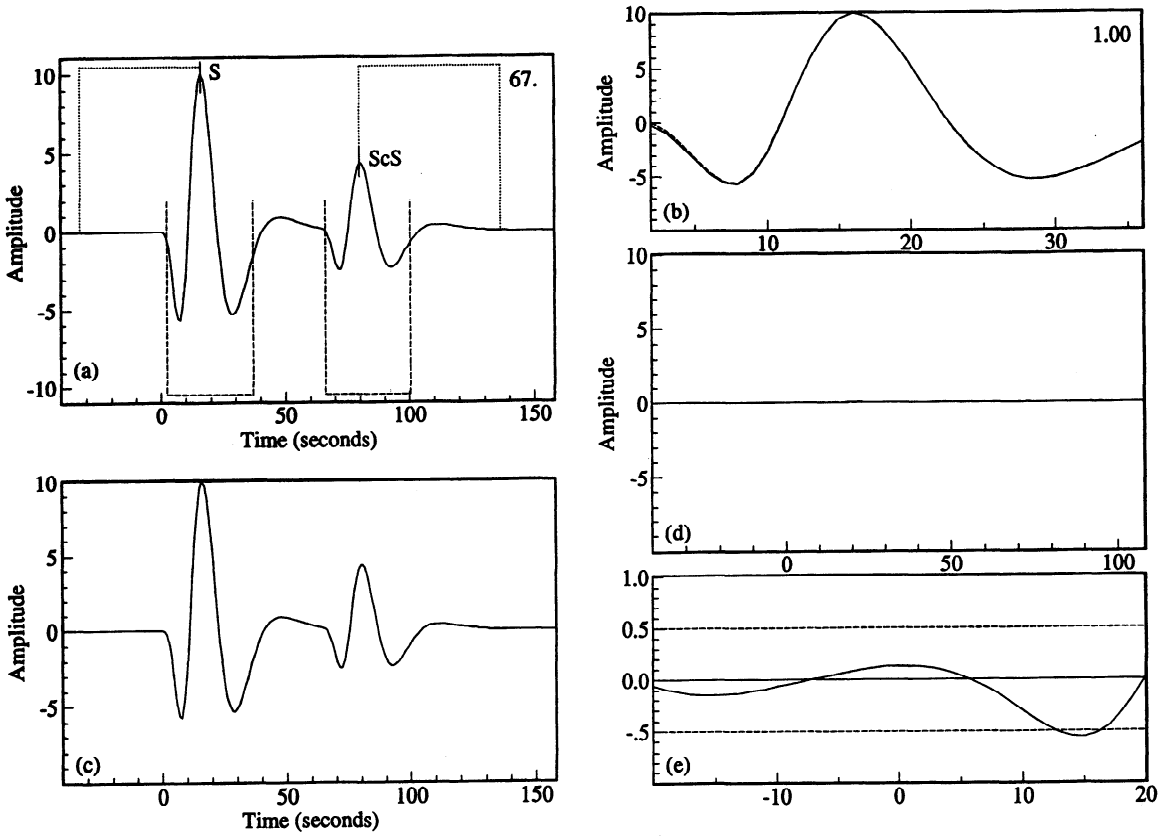

Figure 3. The phase-stripping technique applied to the synthetic SH waveform for the model PREM at an epicentral distance of 67°. See Figure 2 caption for details.

grams where the S-ScS cross correlation is high (Figure 2b), generally above 0.97, are chosen to continue with the next step. Near-source and attenuation variations are assumed to be small if the cross correlation between these phases is high. Seismograms with either shallow sources (< 60 km) or deep sources (> 400 km) are chosen in order to avoid contamination due to depth phases (i.e., sS must not interfere with ScS).

Step 2. The region preceding the S arrival and following the ScS arrival will be unaffected by the D'' signal. Therefore a reference pulse with no D'' signal can be constructed by joining the front portion of the S phase (first dotted interval in Figure 2a) with the trailing portion of the ScS phase (second dotted interval in Figure 2a). The phases are joined at the position of the phase picks (usually the pulse maxima) with the necessary amplitude scaling. The reference pulse half width is at least as wide as the separation between the S and ScS phases. The reference pulse should include any waveform complications due to near-source or near-receiver structure.

Step 3. A composite reference trace is generated by superposing two reference pulses; one is scaled and aligned on the S arrival and the other on the ScS arrival. Figure 2c shows the resulting fit to the synthetic example. Note that both S and ScS are well fit by the reference trace, but that a mismatch exists where the SdS arrival is present in the synthetic seismogram. We isolate the SdS arrival by subtracting the composite reference trace from the seismogram (Figure 2d).

Step 4. The remaining signal (Figure 2d) is cross-correlated with the reference pulse. Strong positive peaks in the cross-correlation function (Figure 2e) are interpreted as indicating an SdS phase.

Figures 2 and 3 illustrate this technique when an SdS phase is both present and absent. The cross-correlation functions clearly indicate when the SdS phase is present. The technique will work as long as noise does not degrade the initial S-ScS cross correlation too much, in which case the procedure fails to get past the first step. Experiments with synthetics for different offsets show that the technique begins to break down at offsets greater than 74°, because the S and ScS phases start interfering with each other and the SdS phase becomes distorted due to the triplication. The technique is not expected to work very well at distances less than 63° because the predicted SdS signal is very weak. As the epicentral distance increases, the technique often works best if a waveform peak toward the end of the S (ScS) phase is picked as the suturing point for the reference pulse. This is because the SdS signal can interfere with the initial portion of the ScS waveform due to the long pulse-widths of the waveforms.

Data Analysis

We have applied the phase-stripping technique to the GDSN long-period SH wave data set that spans recordings from 1976 through 1987 and is distributed by the National Earthquake Information Center (NEIC). This data set contains almost 4000 records with source-receiver distances between 63° and 74°. S versus ScS cross correlations have been calculated for these data in a lower mantle tomography study by *Woodward and Masters* [1991]. We applied our method to only those seismograms *Woodward and Masters* [1991] determined to have a good S versus ScS cross correlation (those that they graded with A or B quality fits); this reduced the data set to 446 seismograms. In order to avoid contamination from depth phases we used only those events with source depths less than 60 km or greater than 400 km; this further reduced the data set to 410 seismograms. The data coverage is shown in Figure 4, where CMB bounce points for the ScS arrivals are plotted. In the northern hemisphere the coverage is especially good beneath Asia, the north Pacific, and the Arctic. There is very poor data coverage in the southern hemisphere, with the exception of the Australasian region.

After phase stripping, a grading system was used to evaluate the quality of the resultant SdS signals. The first step was to decide if an SdS phase was present. This was fairly clear by visual inspection of the resultant waveform and by a strong positive peak in the cross-correlation function. Those signals in which there appeared to be an intermediate phase were further graded A, B, or C depending on the waveform quality. Typically, A quality SdS waveforms had distinct cross-correlation peaks greater than 0.85. The analysis yielded 36 A picks, 85 B picks and 96 C picks. A D'' signal could not be identified for 193 of the studied seismograms. In these cases, there generally was some unaccounted for structure in the waveforms between S and ScS, but no clear pulse similar in shape to the reference pulse. It was generally difficult to determine if this was due to the absence of a D'' reflector, multiple D'' reflectors, or random noise. There is a possibility that some of the ambiguous results could be due to multiple discontinuities in D'', as has been suggested by *Gaherty and Lay* [1992] and *Vidale and Benz* [1993].

An example of an A quality fit for a shallow source is shown in Figure 5 and for a deep source in Figure 6. A typical B quality fit is shown in Figure 7. An example of a case where there was little indication of an intermediate signal is shown in Figure 8. There were many cases where one could not tell whether or not there was any SdS signal present (Figure 9). The initial S-ScS cross correlation was typically not very high for these cases.

Estimating the D''-reflector depth from the resultant S-SdS and ScS-SdS residuals is an inherently nonunique problem. The trade-off between reflector depth and velocity gradients both above and below the reflector allows many possible solutions. Nevertheless, in order to get a simple estimate of D'' thickness, SdS travel times were calculated for a range of modified PREM models with D'' reflectors every 20 km from the CMB. Note that the velocity structure of these models is exactly the same as that for PREM. In other words, we have assumed PREM velocities above and below our hypothetical reflectors. Travel times were also calculated with source depths every 20 km in each of the reflector models. Estimates of D'' thickness were then obtained using a three-dimensional interpolation

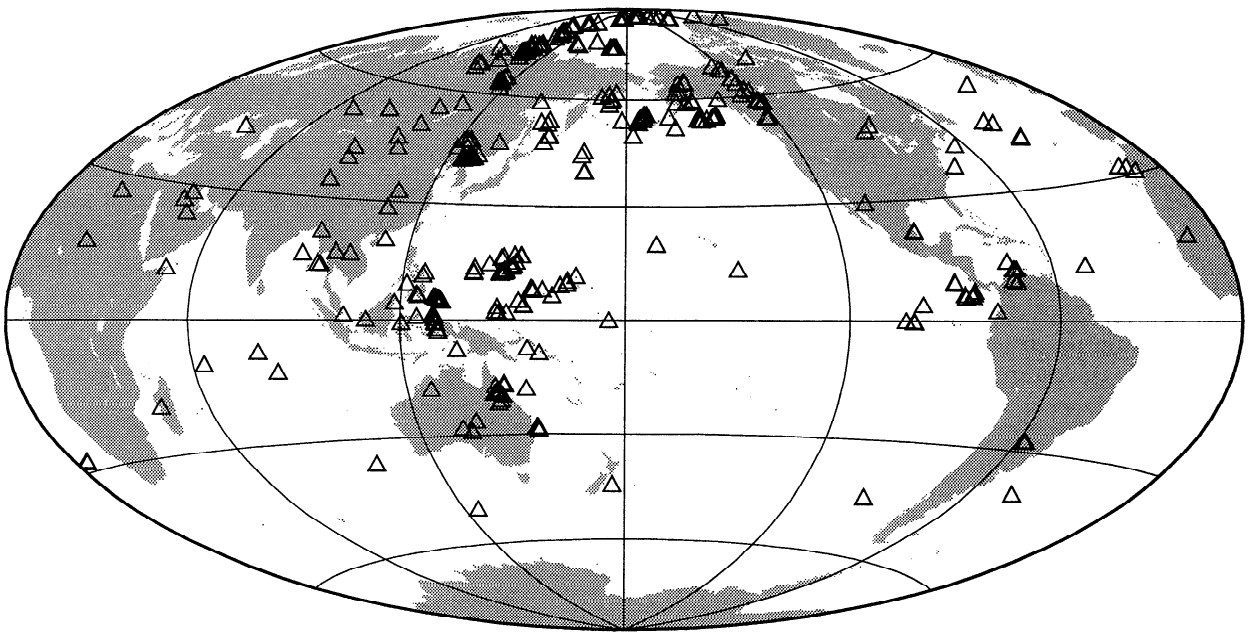

Figure 4. Areal coverage of the data used in this study. Triangles are plotted at the surface projections of the ScS bounce points (variations in source depths are taken into account).

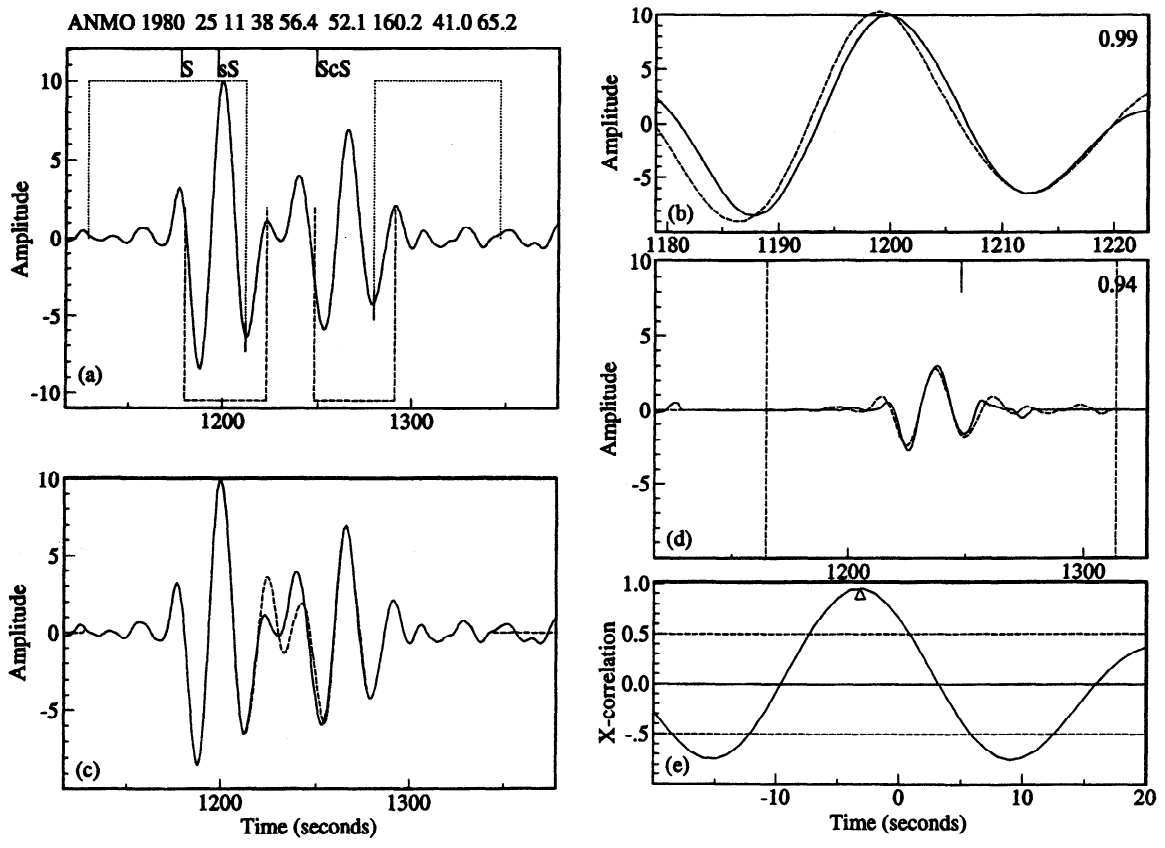

Figure 5. An example of the application of the phase-stripping technique where the resultant *SdS* waveform fit with the reference pulse is given an A quality grade. The example is for a shallow source (41 km). The source and station information is given above Figure 5a in the following order: station name, event year, Julian date, hours, minutes and seconds, event latitude and longitude, source depth, and source-station epicentral distance. See Figure 2 caption for details. The PREM predicted *S*, *sS*, and *ScS* picks are shown in Figure 5a. In Figure 5d the cross-correlation window is bracketed by dotted lines, and the *SdS* time pick is indicated by a triangle at the top of the window.

between epicentral distance, source depth, and reflector depth for given *ScS-SdS* and *S-SdS* residuals. The average of the depths predicted by *ScS-SdS* and *S-SdS* travel-times was then used as our final depth estimate. Note that the *ScS-SdS* and *S-SdS* depth estimates will differ somewhat due to differences between our simple reflector models and the actual velocity structure across the D'' discontinuity. Using the average depth estimate mitigates the differences somewhat; however, the uncertainties in computed D'' depths introduced by these differences are fairly small compared to the overall spread in the depths. The average difference between each *ScS-SdS* and *S-SdS* depth estimate for all of the A and B picks is 25 km (standard deviation is 18 km).

Results

SdS phases have been identified in five regions using the phase-stripping technique. Most of these areas have been examined in previous studies. In general, our results indicate that it is difficult to explain these phases as reflections from a continuous horizontal reflector; rather, they suggest that the top of the D'' region can be quite variable even within particular regions.

North Central Asia

The area of D'' beneath northern Eurasia has been the subject of many previous studies because of its favorable position between northwest Pacific events and European stations. Using *S* waveforms, *Lay and Helmberger* [1983] estimated that the D'' layer is almost 320 km thick in northwestern Siberia. *Gaherty and Lay* [1992] studied a broader region of Eurasia and found their data best supported a shear-velocity model with a D'' discontinuity 290 km above the CMB. *Weber and Davis* [1990] observed *P* waveforms recorded at the Gräfenberg array (GRF) and also estimated a 290-km-thick reflector under northern Siberia. They also showed that this reflector is not visible in a region a few hundred kilometers away. Northwest of the Weber and Davis study area, *Houard and Nataf* [1992] used data from the Laboratoire de Detection Geophysique (LDG) network to interpret a similar reflector, but found that the data suggested the possibility of undulations in the

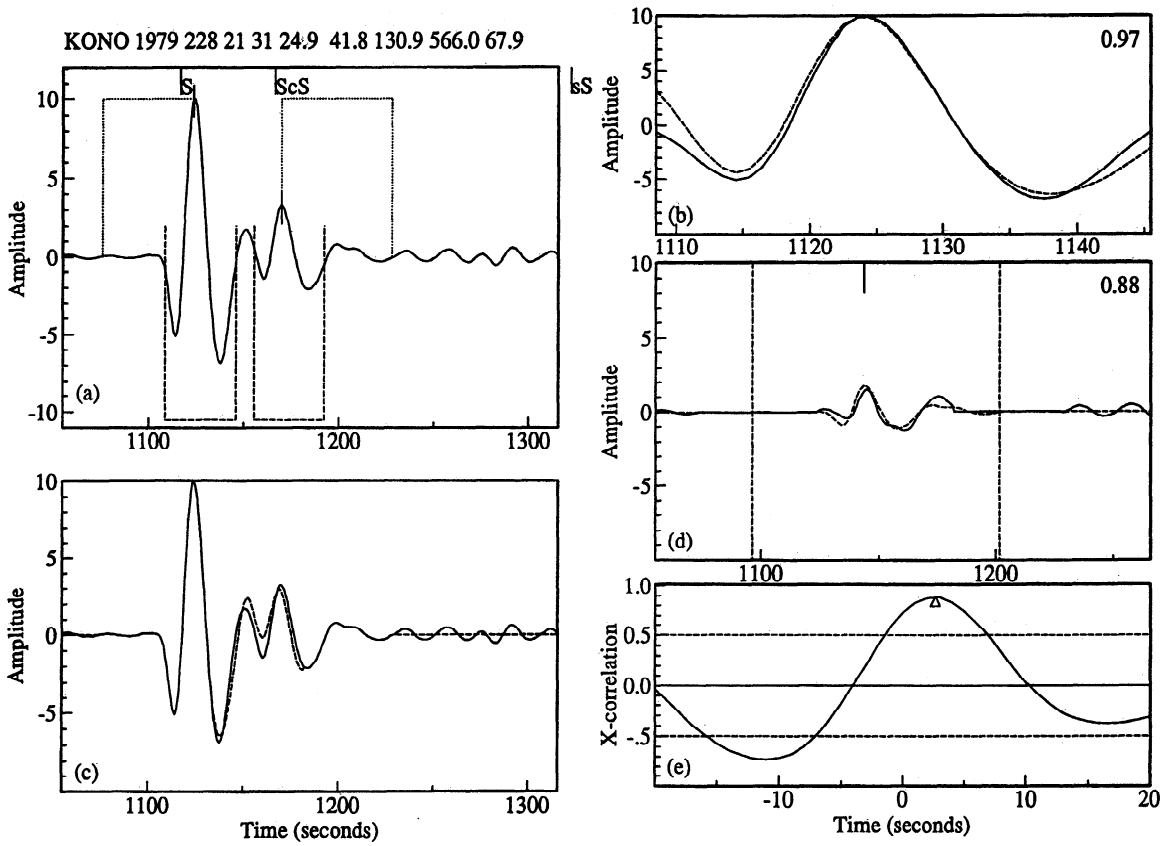

Figure 6. An example of the application of the phase-stripping technique where the resultant SdS waveform fit with the reference pulse is given an A quality grade and the source is deep (566 km). See Figure 5 caption for further details.

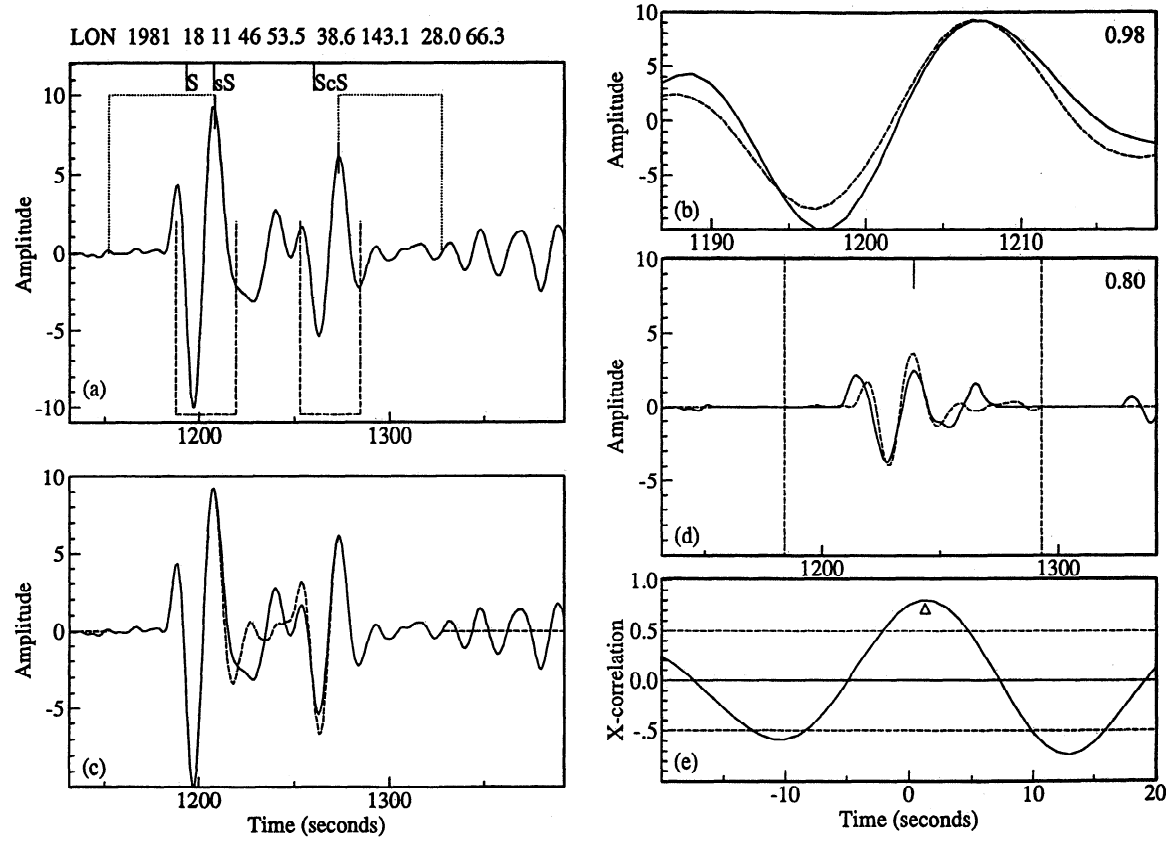

Figure 7. An example of the application of the phase-stripping technique where the resultant SdS waveform fit with the reference pulse is given an B quality grade (SdS cross correlation typically less than 0.85). See Figure 5 caption for further details.

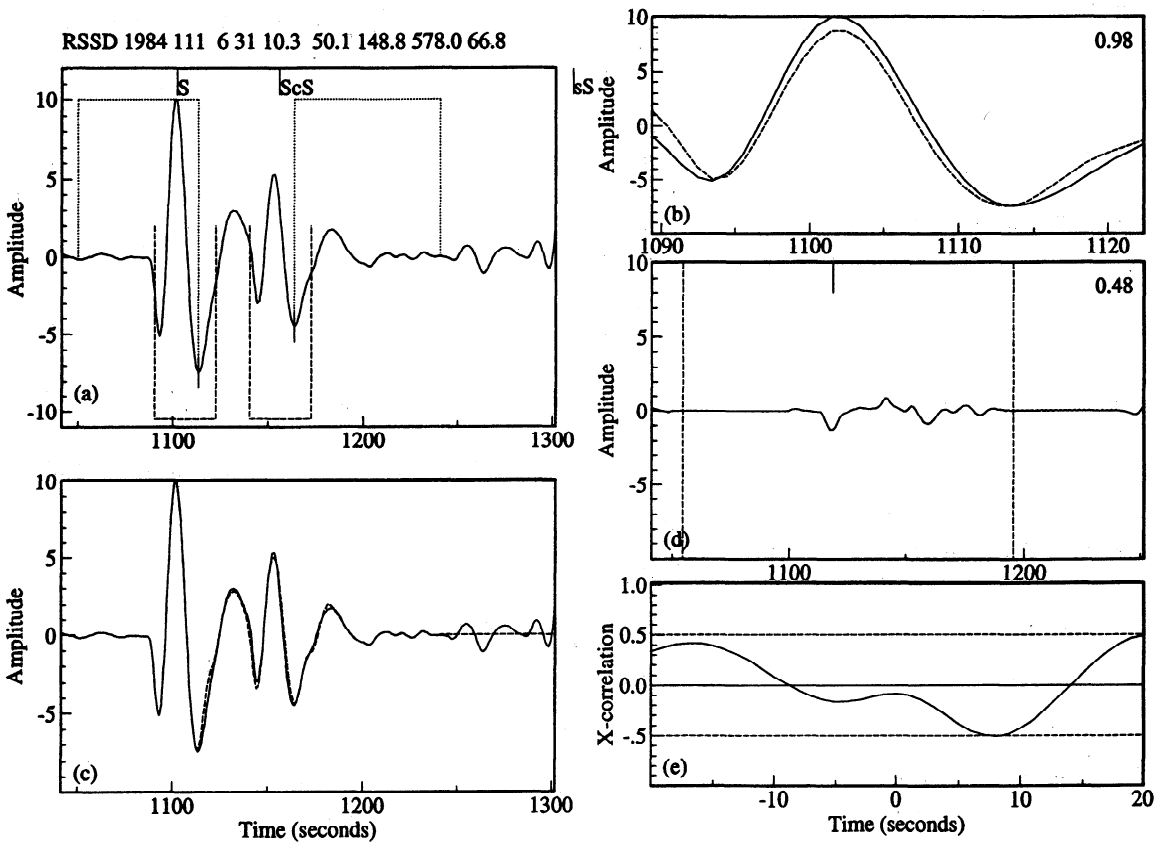

Figure 8. An example of the application of the phase-stripping technique where there is no apparent resultant D'' signal. See Figure 5 caption for further details.

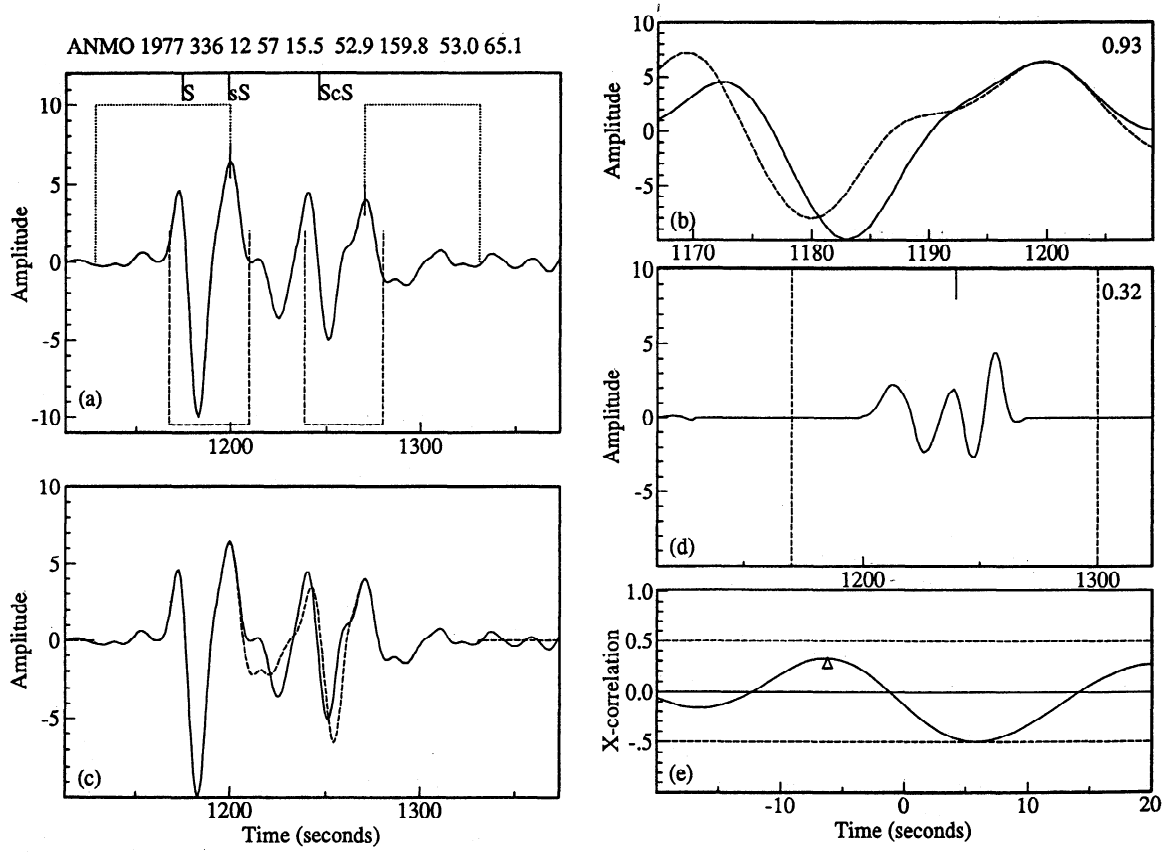

Figure 9. An example of the application the phase-stripping technique where it is not clear whether or not a D'' signal is present. See Figure 5 caption for further details.

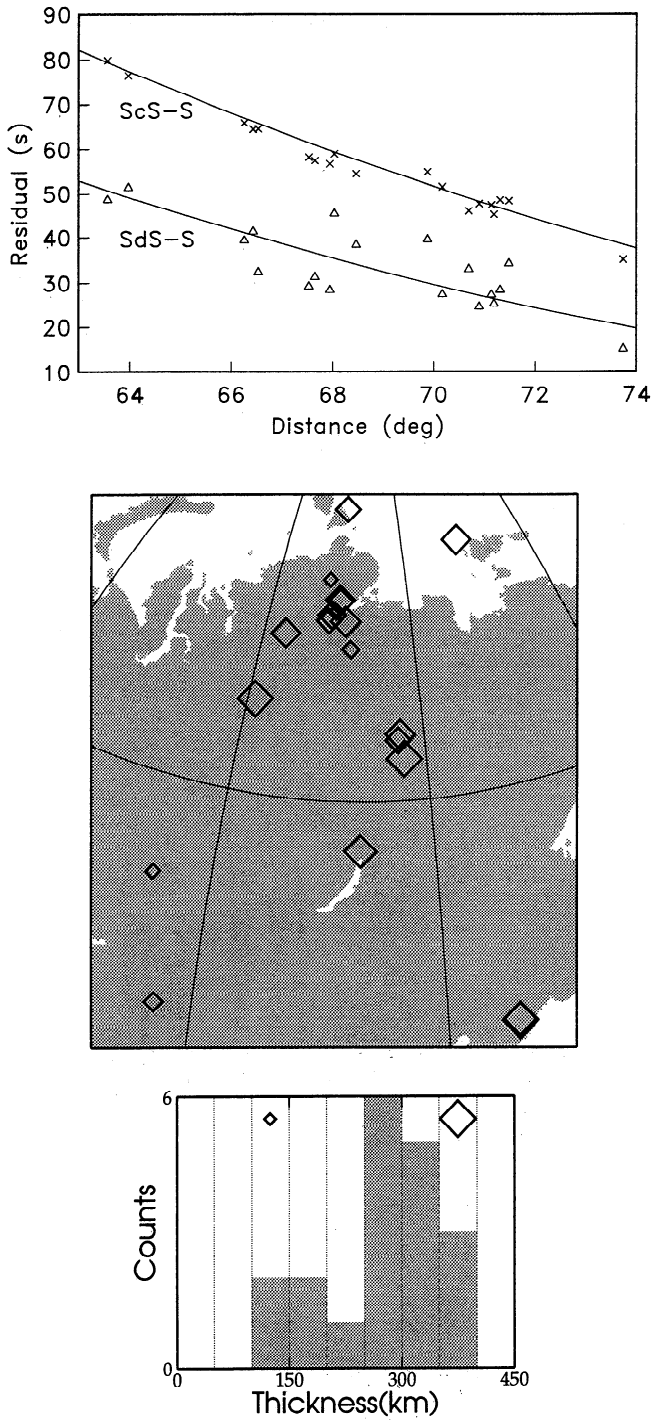

Figure 10. The results summarized for the area beneath central Asia (40°-80°N and 80°-130°E). (top) Depth-corrected travel-times residuals with respect to S for A and B picks. The solid lines are the predicted residuals for the model SGLE [*Gaherty and Lay*, 1992]. (middle) Stereographic equal-area projection showing the surface projections of the SdS bounce points and interpreted D'' thicknesses. (bottom) Histogram shows the thickness distribution and indicates the scale for the diamond symbols used in the map projection.

reflector. *Weber* [1993] studied both P and S arrivals at GRF and, confirming the results of *Weber and Davis* [1990], found D'' reflections were not always observed in this area. Furthermore, he found a region where SdS reflections, but not PdP were observed. Again in northern Siberia, *Baumgardt* [1989] analyzed P waveforms and predicted a D'' reflector at 344 km above the CMB. He also noted that there were wide variations in the amplitudes of D'' reflections and, in places, D'' reflections were unobservable, suggesting strong lateral variations in D''. Considering north central Asia more generally, *Weber and Körnig* [1992] used P wave data from the bulletins of the International Seismological Center to predict, on average, a 230-km-thick D'' region, but with considerable regional variability in this thickness.

The ScS-S and SdS-S residuals, as a function of epicentral distance, for our A and B picks with bounce points in north central Asia are shown in Figure 10. For reference the travel time curves for the *Gaherty and Lay* [1992] model SGLE are shown. In general, the SdS residuals cluster around the SGLE prediction, but do indicate some variability from this model. Figure 10 also shows the variations in thickness estimates for this region. The 19 estimates of D'' thickness range between 140 km and 370 km with an average thickness of 270 km. In agreement with previous studies, northern Siberia shows considerable variability in thickness.

Alaska

Alaska is another well-studied region because it lies midway between northwest Pacific events and North American stations. *Lay and Helmberger* [1983] estimated a shear-velocity discontinuity 278±25 km above the CMB in this region. *Young and Lay* [1990] refined this work, predicting D'' to be 243 km thick in this area. In contrast, *Young and Lay* [1989] found no evidence of a P wave reflector for this region. More recently, *Weber and Körnig* [1992] observed considerable variability in D'' thickness throughout this region (260±100 km) and even found striplike regions of no apparent P wave reflection.

Figure 11 shows the travel-time residuals, relative to S, for the region under Alaska. Once again, the residuals for the model SGLE [*Gaherty and Lay*, 1992] are shown as a reference level. The residuals form a loosely coherent pattern for the region. Thickness estimates of D'' are also plotted in Figure 11. The average thickness for the region from 16 observations is 296 km, but D'' ranges dramatically from 160 km thick to over 375 km thick. There is a very strong spatial correlation for the residuals with bounce points under the Aleutians near 185°E, 53°N. The estimated D'' thickness in this area from six observations is 375±25 km. There seems to be a thinning in D'' between 55°N and 60°N, although the data are too sparse to say anything conclusive.

Arctic

The Arctic region has been examined in studies primarily by Weber and coworkers. *Weber and Davis* [1990] found evidence of a D'' discontinuity under the Lomonosov ridge and possibly under northern Greenland, but not throughout the Arctic region. The study of *Weber and Körnig* [1992] gave similar results (average D'' thickness of 230 km). *Weber* [1993] further

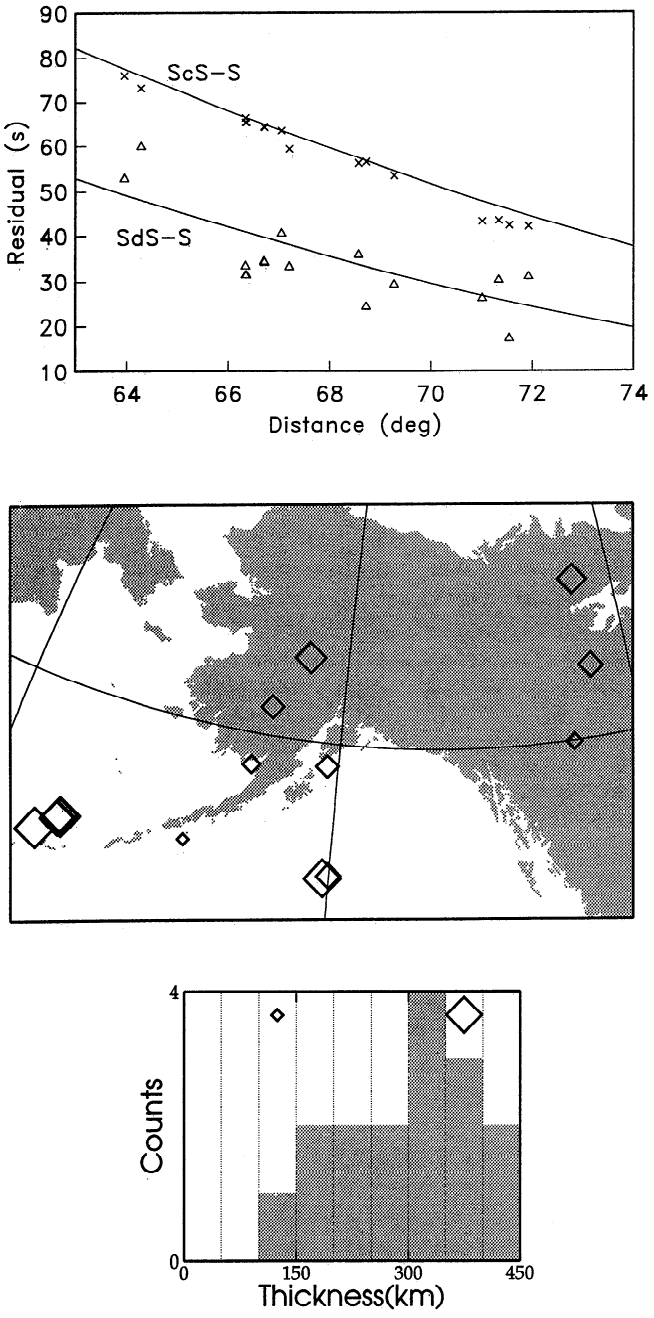

Figure 11. As in Figure 10, but for the area beneath Alaska (50°-70°N and 180°-240°E).

studied this region and found a 280-km-thick D'' layer under the Nansen basin that is a good reflector of P waves, but a weak reflector of S waves. He also found that under the Kara Sea D'' is a good P-wave reflector, but not an S-wave reflector. *Vidale and Benz* [1993] studied P waves from a Chinese nuclear test and found D'' reflections from a laterally isolated discontinuity 130 km above the CMB and, consequently, suggested layering within D''(the published bounce points of *Vidale and Benz* [1993] should be farther west, beneath the east Siberian Sea as shown by Nataf and Houard [1993]). Finally, *Krüger et al.* [1993] found that in a region near the Nansen basin, just north of Severnaya Zemlya, D'' thinned to less than 200 km. In fact, using a double-beam summation technique they observed, well within the Fresnel zone, a D'' variation in this region of nearly 50 km.

Once again the travel time residuals for this region show reasonable coherence (Figure 12). Thickness estimates for the 20 observations in this region yield an average D'' thickness of 268 km. Many of the observed reflections lie directly under the Lomonosov ridge. The absence of reflections beneath the Nansen basin and

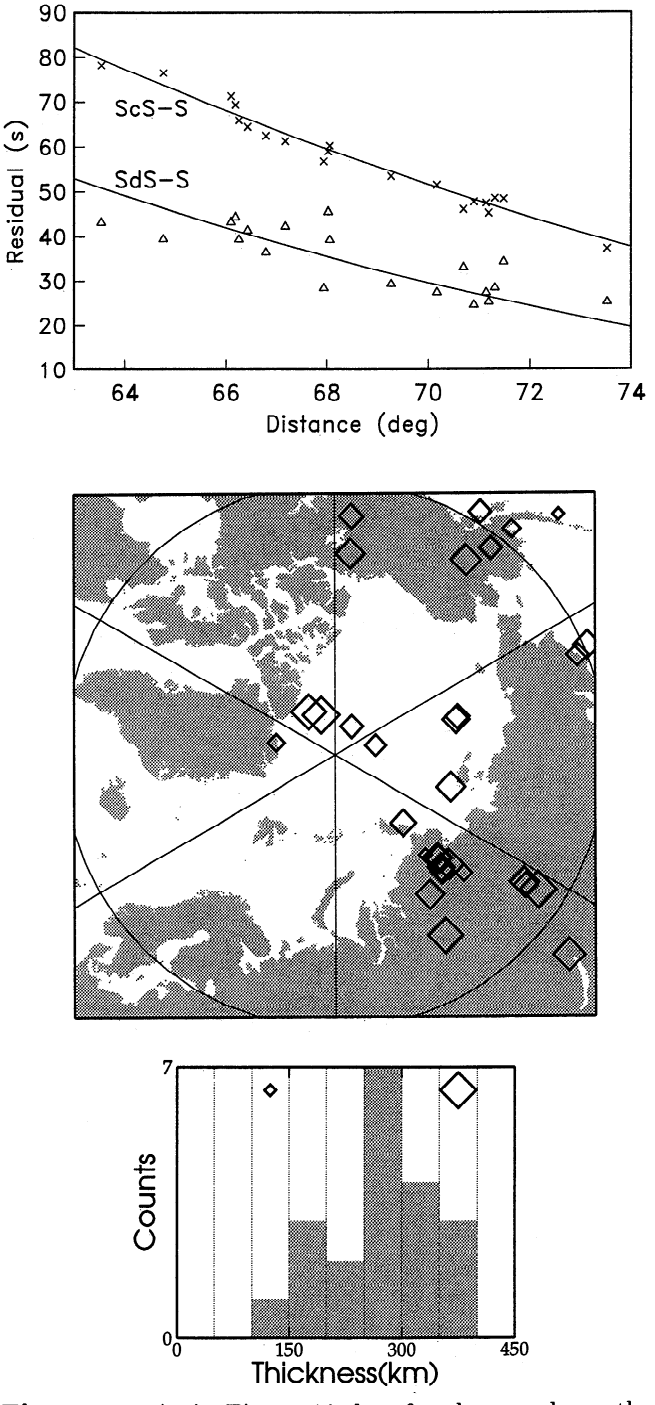

Figure 12. As in Figure 10, but for the area beneath the Arctic (north of 66°).

Kara Sea are in agreement with *Weber's* [1993] findings.

Australasia

The D'' region under Australia and the western Pacific to the north appears to be quite complex. *Wright et al.* [1985] found evidence for a P wave discontinuity roughly 200 km above the CMB based on a sharp change in the slownesses of arrivals with epicentral distances between 85° and 88°, but *Weber and Körnig* [1992] found little evidence for a P wave discontinuity in this area. On the basis of long-period ScS reverberations, *Revenaugh and Jordan* [1991] identified a D'' reflector that is on average 325 km (270 km to 340 km) above the CMB through part, but not all of this region. *Garnero et al.* [1993] suggested an S wave reflector about 280 km above the CMB in a region northeast of Papua New Guinea. Using core-diffracted phases, *Wysession et al.* [1992] found evidence of notably strong variations in D'' velocities and in Poisson's ratio in the region beneath Indonesia.

The travel time residuals observed in our study are shown in Figure 13 together with the thickness estimates. The travel time residuals suggest that the average thickness for D'' in this region should be thin in comparison to SGLE, and, in fact, the depth estimates give an average value for 27 observations of 245 km. This average is a little misleading because there is a definite trend of thickening toward the east (Figure 13). Although the coverage is sparse, there is some spatial coherency in these depth estimates in the region near 155°E, 30°S where five observations predict a thickness of roughly 300±40 km.

West of Central America

The final region studied is the CMB area below the Cocos plate, west of Central America. *Lay and Helmberger* [1983] estimated a 250-km-thick D'' layer in this region using S waveforms. *Weber and Körnig* [1992] found strong evidence for a P wave discontinuity 340 km above the CMB, but found that the discontinuity was not present throughout the region. *Garnero et al.* [1988] suggested the absence of a D'' discontinuity farther west into the Pacific, but *Garnero et al.* [1993] refined this work and found evidence for a relatively thin (180 km thick) D'' reflector in a region southeast of Hawaii.

We have very poor coverage for this area, but for comparative purposes the results are presented. Figure 14 shows the travel time residuals and thickness estimates for the area. The results agree somewhat with those of *Weber and Körnig* [1992].

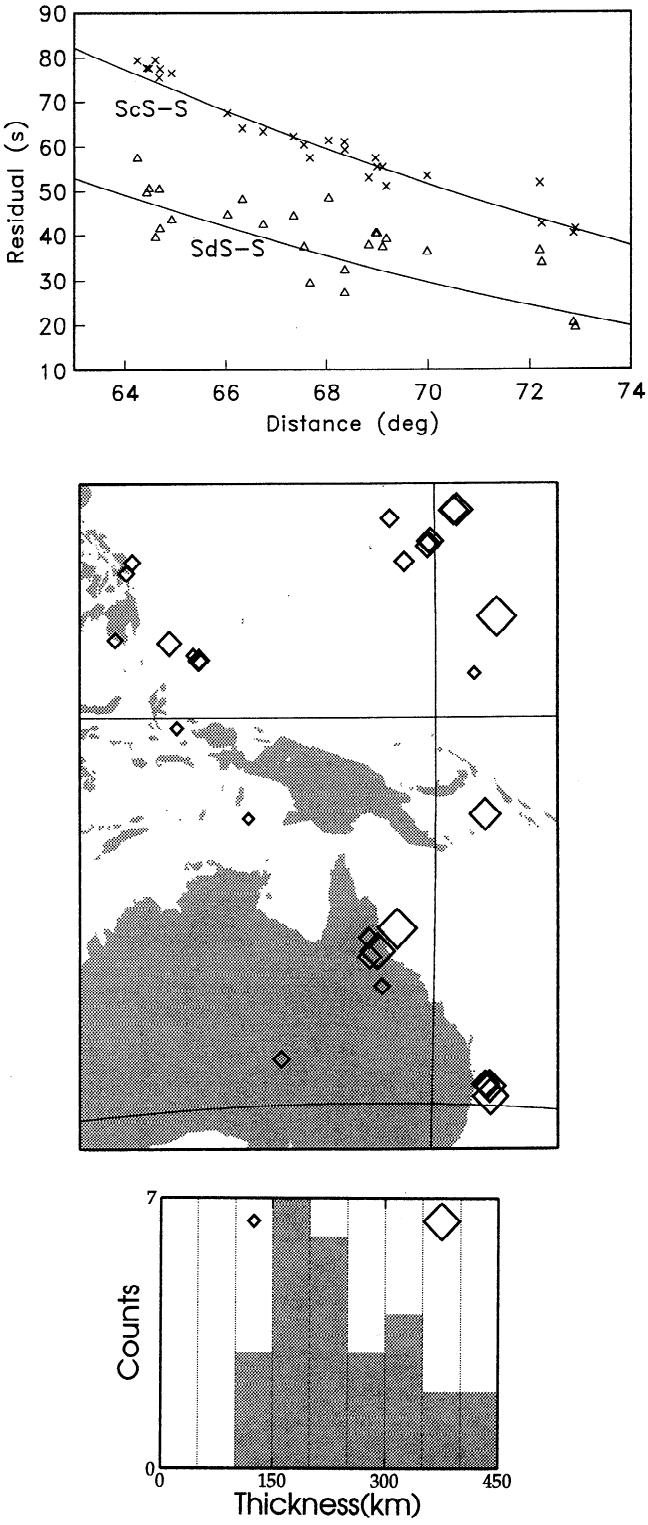

Figure 13. As in Figure 10, but for the area beneath Australia and the western Pacific (−30°-20°N and 130°-160°E).

Discussion

The analysis of 12 years of GDSN data using the phase-stripping technique has enabled localized estimates of D'' thickness in regions where the upper boundary of the layer is a discontinuity. Figure 15 shows a histogram of predicted D'' thicknesses for the entire data set. The average thickness is 260 km, but there is a fairly uniform distribution between 150 km and 350 km with a sharp taper beyond these thicknesses. At least some of this taper is probably due to the difficulty of observing SdS at times close to S or ScS in the long-period data. Figure 16 shows our thick-

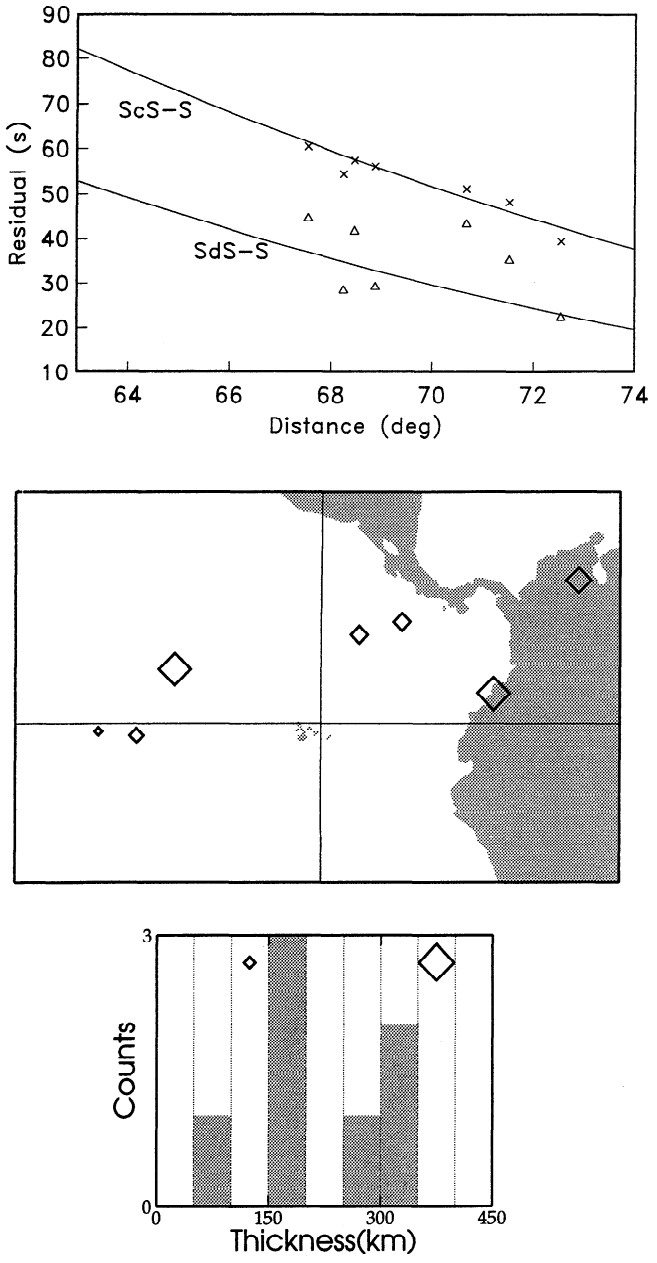

Figure 14. As in Figure 10, but for the area beneath Central America and the Cocos plate (−5°-10°N and 255°-290°E). Note that A, B, and C picks are used in this region.

ness estimates compared to those of previous studies for particular regions. Our results generally lie within the scatter shown by previous observations, but it appears that a wide range of thicknesses are present (even within each region) implying considerable lateral variation in D'' structure.

The data as a whole can be used to generate a large-scale map of D'' topography (Figure 17). This is by no means a global map because there are many large areas where there are no data. The results have been smoothed using 5° cap averages within the regions of data coverage. The sparse global coverage and scatter in the estimated depths make interpretation of this map difficult. Some of the points plotted (e.g. near

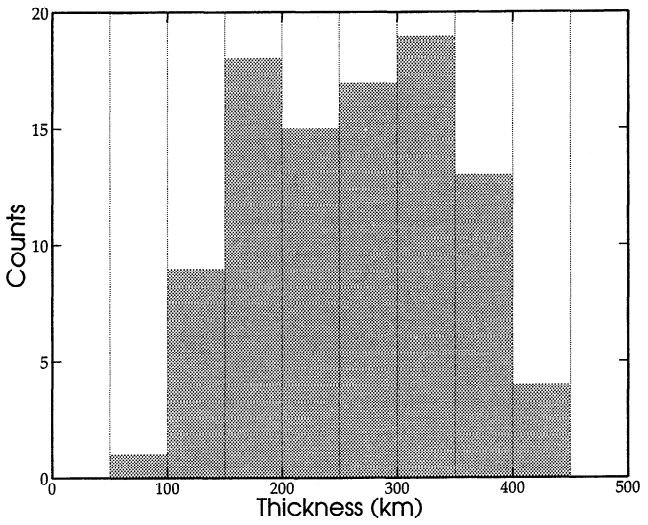

Figure 15. Histogram showing the distribution of estimated D'' thicknesses for the A and B quality picks of the entire data set.

Africa, Hawaii and eastern North America) are defined by so few seismograms that the D'' depth estimates should be considered extremely tentative. The areas of observed D'' reflections correlate closely with the raw data coverage (compare Figures 4 and 17). This reflects the fact that we were unable to identify specific regions which consistently gave null observations for D'', although many individual seismograms did not show clear D'' signals. Within the areas of data coverage, there is some spatial correlation between the thickness measurements. A region of thick D'' can be seen beneath the rim of the western and northern Pacific. This layer seems to thin moving westward into Australia and

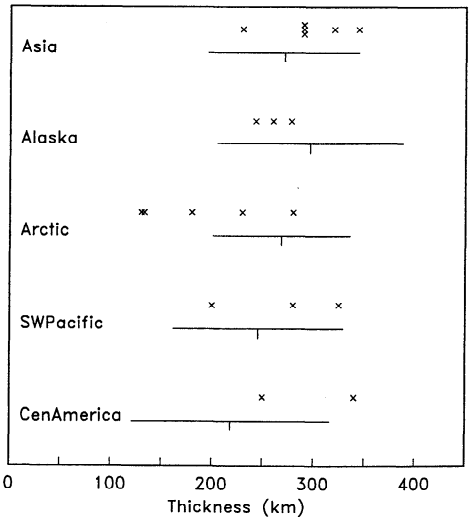

Figure 16. A comparison by region of estimated D'' thicknesses for this study with those of previous studies. The horizontal lines extend one standard deviation from the average regional thickness values (vertical ticks) estimated in this study. The crosses indicate predictions from previous studies (see text for references).

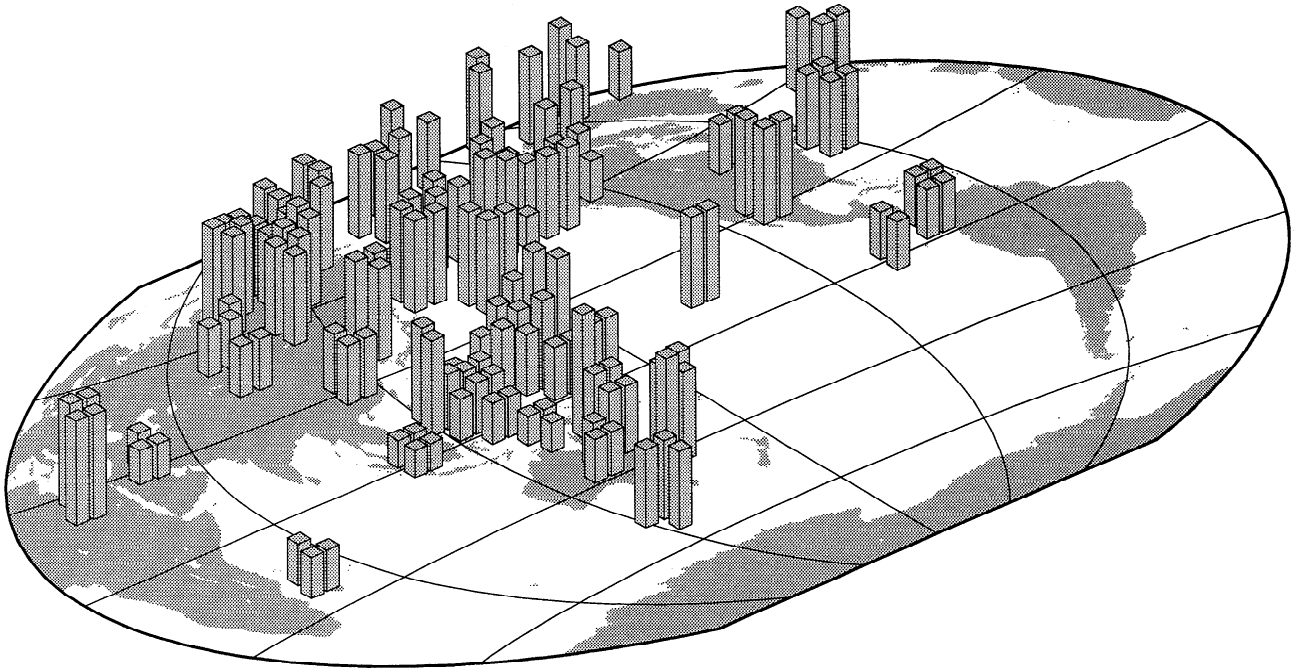

Figure 17. A large-scale map of D'' topography. Individual D'' thickness estimates have been smoothed with a 5° cap average, and the map projection is a Winkel-Tripel [*Wessel and Smith*, 1991].

Asia. The thick D'' region roughly correlates with current subduction regions.

Most recent mantle tomography models are in approximate agreement in their lowermost mantle S velocity structure [e.g., *Masters et al.*, 1992; *Woodward et al.*, 1993]. Figure 18 shows a comparison between the lower mantle velocity anomalies for one of these models (SH10C of *Masters et al.* [1992]) and our smoothed D'' thicknesses. In general, the well-sampled areas of our SdS data coverage correspond to fast regions in the tomography models. A notable exception is the region just north of the equator and near 160°E. Our results suggest that D'' is roughly 300 km thick and a good reflector of S waves in this region, whereas SH10C [*Masters et al.*, 1992] and WM13 [*Woodward et al.*, 1993] indicate that the lower 300 km of mantle in this area is a lateral transition region from high to low velocities. A normal or thicker than normal D'' layer in this region has also been suggested by *Garnero et al.* [1993] and *Revenaugh and Jordan* [1991]. There appears to be some tendency for D'' to be thinner in the areas of highest S wave velocity (e.g., beneath western Australia, Sumatra, and China) and to thicken as it moves away from these areas. This trend is consistent with the inverse correlation between lowermost mantle velocity and D'' thickness noted by *Revenaugh and Jordan* [1991] using ScS reverberation data in this area.

If this pattern is real, a possible explanation may involve the flow regime in the lowermost mantle. In general, one would expect the fast regions in the lowermost mantle to be areas of downwelling, the slow areas to be areas of upwelling, and the transition regions to be characterized by horizontal flow. The recent convection calculations of *Phipps Morgan and Shearer* [1993], based on the S wave tomographic models, are consistent with this overall pattern and exhibit a weak correlation (particularly in the western Pacific) with the D'' thicknesses shown in Figure 18. Thus it is possible that downwelling high-velocity material is depressing the D'' boundary, but as the material flows horizontally toward upwelling regions the D'' layer thickens and warms. In the warmest regions of the lowermost mantle, the thickness of D'' is currently extremely uncertain due to a lack of observations. The layer may continue to thicken, or, alternatively, the material may warm to a point that the velocity contrast across D'' is reduced or eliminated, thus limiting seismic observations of D'' in these regions.

This scenario is similar to that hypothesized by *Revenaugh and Jordan* [1991]; their model suggests that a discontinuity atop a thickening D'' layer will be preserved into the upwelling region, in which case the southern Pacific should be characterized by an anomalously thick D'' layer. *Garnero et al.* [1993] found evidence for a D'' discontinuity only 180 km thick beneath a small patch of the Pacific southeast of Hawaii. However, this patch is within a slow-to-fast transition region in the tomography models, outside of the main slow anomaly in the southern Pacific. More data coverage in the southern Pacific will be necessary to help resolve these issues. It is unfortunate that we could not confidently identify regions lacking a D'' discontinuity and that our regions of D'' reflections are essentially defined by the data coverage.

It is important to consider whether the anomalous ScS precursors extracted from the data could be ex-

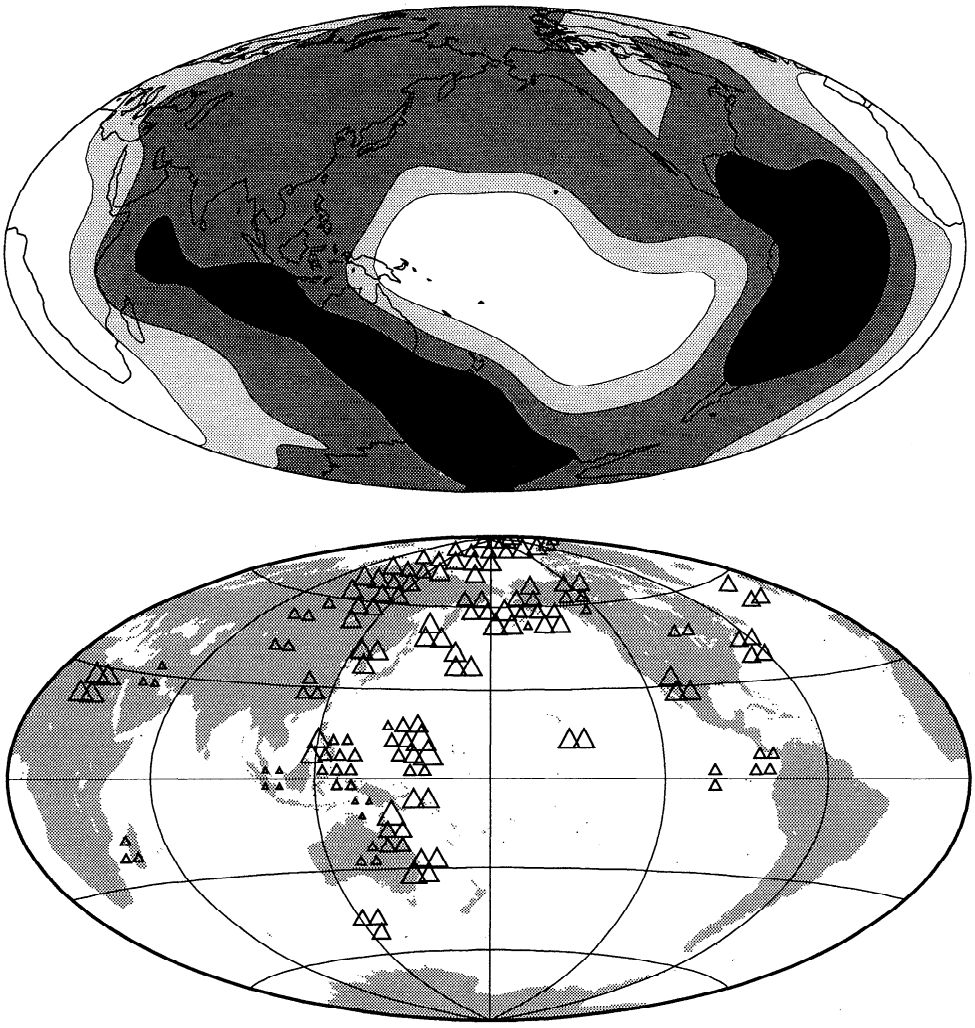

Figure 18. A comparison of estimated D'' thicknesses and lower mantle S wave velocities described by the model SH10C of *Masters et al.* [1992]. Individual D'' thickness estimates have been smoothed with a 5° cap average (bottom). The velocity contours (top) vary from black indicating a velocity anomaly >1% to white indicating a velocity anomaly <-1%.

plained by mechanisms other than D'' reflections. We have mitigated the possibility of erroneous interpretation due to attenuation and near-source variations in S and ScS by requiring strong correlation between the phases at the onset of the phase-stripping technique. Synthetic SH waveforms have shown that the time window between S and ScS and just beyond ScS, at epicentral distances between 60° and 75°, should be almost devoid of secondary phases due to standard one-dimensional Earth structure other than D'' reflections (there may be some contamination due to the underside 660-km reflected phase, $S660S$, at ranges below about 67°, but this phase is much weaker than the predicted SdS amplitudes). No secondary phases should follow the ScS arrival except for the underside D'' reflection, $SDDS$, which synthetics indicate is too weak to be observable.

Could our observed D'' arrivals be a result of random noise in the seismic data which contaminates the region between S and ScS? This explanation seems unlikely, given the often excellent fits between SdS and the reference pulse, the rough spatial coherence of our results, and the fact that the D'' signals almost always show positive correlations with the reference pulses. If the signals were pure noise one would expect not only poor reference pulse correlations, but also as many negative correlations as positive ones.

There is the possibility of secondary arrivals due to slab multipathing, especially in regions along strike from subduction regions [*Kendall and Thomson*, 1993]. In order to get multipathing, rays must travel through a wavefront caustic. A travel time triplication will ensue and rays on the reverse branch of this triplication will be Hilbert-transformed. The time separation between branches for a generic slab model is of the order of a few seconds [*Kendall and Thomson*, 1993]. This small travel time triplication distorts and broadens long-period waveforms, making it virtually impossible to distinguish separate branch arrivals. This effect is intimately related to the slab diffraction effect described

by *Cormier* [1989]. It is possible that an S waveform and not the ScS waveform may exhibit multipathing effects, but in such a case the S and ScS waveforms would cross-correlate poorly and the event would not be used in our analysis. Furthermore, our observed ScS precursors are always tens of seconds after the S arrival and do not resemble Hilbert transforms of the reference pulse (in which case they would correlate poorly with the reference pulse). Finally, the effects of slab multipathing should exhibit a strong correlation with source depth and receiver azimuth, but our results show no such correlation.

It has been proposed that small-scale discrete scatterers could produce anomalous energy as an ScS precursor [*Haddon and Buchbinder*, 1987]. The variability of our results across regions certainly suggests strongly heterogeneous structure in the lower mantle. The rough spatial coherency of our results, though, suggests some large-scale variations in this structure. Evidence of small-scale heterogeneity within D'' [e.g., *Bataille and Flatté*, 1988; *Kruger et al.*, 1993] from high-frequency data implies that D'' can scatter seismic energy. Using long-period data enables the mapping of larger-scale variations in this structure which may initially provide a more useful constraint for global geodynamics.

An attractive feature of our analysis is that each of our depth estimates can be thought of as spot measurements of D''. In many previous studies, people have precluded the possibility of seeing regional variations in D'' by using single horizontal reflector models to interpret the data. Our results help explain the wide range of interpreted D'' depths within given regions in previous studies (e.g., north central Asia, Figure 16). The size of our imaged spot on D'' is controlled by the Fresnel zone. The Fresnel footprint for long-period S waves is of the order of 5°-10°, but our results show variations in D'' thickness on a finer scale. Though curious, this result is often observed in other studies. For example, *Kruger et al.* [1993] observe variations in D'' well within the Fresnel zone resolution and infer that D'' velocity structure is strongly inhomogeneous on a fine scale. Strong heterogeneity will cause interference effects and change the shape of the wavefront and, consequently, the size of the Fresnel region. There is also the possibility of bounce point mislocations due to topography on D'' and lateral velocity variations in the lower mantle. Finally, there is the possibility of multiple layering within D'' [e.g., *Vidale and Benz*, 1993] with our technique latching onto different depths depending upon the relative amplitude of the reflections. It is clear that D'' is a complex region, characterized by strong lateral heterogeneity and abrupt velocity gradients. Unraveling all of these complexities will be a considerable challenge. A useful step in this process will be to explore the sensitivity of waveforms and Fresnel regions to D'' structure by calculating Maslov synthetic waveforms (for example) for a range of models.

We had hoped that amplitude information could be used to estimate the impedance contrast at D''. However, the amplitudes of our observed SdS phases are highly variable, making it impossible to interpret them with any confidence. Such variability has been observed by others [e.g., *Baumgardt*, 1989], and we often observed amplitudes much larger than those predicted for the model SGLE [*Gaherty and Lay*, 1992]. Because amplitudes are more sensitive than travel times to fine velocity structure, and given the apparent variability in D'' structure, it is not surprising that the amplitudes vary so strongly.

The results presented here can be augmented as long-period waveform data sets continue to grow and as additional stations improve the spatial coverage of ScS bounce points. To enlarge the limited coverage of this study a great many more seismograms must be analyzed. The success ratio of the phase-stripping method is quite low, with only very high quality seismograms giving usable results. The technique itself is somewhat novel and there is potential for it to be applied to other seismological studies.

Acknowledgments. Guy Masters is thanked for providing the presorted ScS-S data set, the cap-averaging software, and constructive advice. Jason Phipps Morgan is thanked for helpful comments and discussions about lower mantle flow and structure. Advice and comments from Michael Weber are greatly appreciated. Paul Wessel and Walter Smith are acknowledged for developing the mapping software GMT used to generate many of the figures. We thank H. Houston, T. Lay, M. Wysession, and E. Garnero for thorough reviews. This research was supported by funding from NSF grant EAR-91-18309, a NSERC Canada postdoctoral fellowship, and the Cecil and Ida Green Foundation.

References

Bataille, K., and S. M. Flatté, Inhomogeneities near the core-mantle boundary inferred from short-period scattered PKP waves recorded at the global digital seismic network, *J. Geophys. Res.*, *93*, 15,057-15,064, 1988.

Baumgardt, D. R., Evidence for a P-wave velocity anomaly in D'', *Geophys. Res. Lett.*, *16*, 657-660, 1989.

Bolton, H. F., and T. G. Masters, S/P ratios in the lower mantle, *Eos Trans. AGU, 73 (43)*, Fall Meeting Suppl., 403, 1992.

Buchbinder, G. G. R., Search for PdP phases using the Yellowknife NWT array, *Eos Trans. AGU, 72 (17)*, Spring Meeting Suppl., 202, 1991.

Bullen, K. E., Compressibility-pressure hypothesis abd the Earth's interior, *Mon. Not. R. Astron. Soc. Geophys. Suppl.*, *5*, 355-368, 1949.

Chapman, C. H., A new method for computing synthetic seismograms, *Geophys. J. R. Astron. Soc.*, *16*, 81-85, 1978.

Christensen, U. R., Models of mantle convection: One or several layers, *Philos. Trans. R. Soc. London A*, *328*, 417-424, 1989.

Cormier, V. F., Some problems with S, SKS and ScS observations and implications for the structure of the base of the mantle and the outer core, *J. Geophys.*, *57*, 14-22, 1985.

Cormier, V. F., Slab diffraction of S-waves, *J. Geophys. Res.*, *94*, 3006-3024, 1989.

Dziewonski, A. M., and D. L. Anderson, Preliminary reference Earth model, *Phys. Earth Planet. Inter.*, *25*, 297-356, 1981.

Elasser, W. M., P. Olson, and P. D. Marsh, The depth of mantle convection, *J. Geophys. Res.*, *84*, 147-155, 1979.

Gaherty, J. B., and T. Lay, Investigation of laterally heterogeneous shear velocity structure in D'' beneath Eurasia, *J. Geophys. Res.*, *97*, 417-435, 1992.

Garnero, E., D. Helmberger, and G. Engen, Lateral variations near the core-mantle boundary, *Geophys. Res. Lett.*, *15*, 609-612, 1988.

Garnero, E. J., D. V. Helmberger, and S. Grand, Preliminary evidence for a lower mantle shear wave velocity discontinuity beneath the central Pacific, *Phys. Earth Planet. Inter.*, *79*, 335-347, 1993.

Gutenberg, B., Über Erdbebenwellen VIIA. Beobachtungen an Registrierungen von Fernbeben in Göttingen und Folgerungen über die Konstitution des Erdkörpers. *Nachr. Ges. Wiss. Göttingen Math. Phys. Kl.*, 125-177, 1914.

Haddon, R. A. W., and G. G. R. Buchbinder, S-wave scattering by 3-D heterogeneities at the base of the mantle, *Geophys. Res. Lett.*, *14*, 891-894, 1987.

Houard, S., and H-C. Nataf, Further evidence for the "Lay discontinuity" beneath northern Siberia and the North Atlantic from short period P-waves recorded in France, *Phys. Earth Planet. Inter.*, *72*, 264-275, 1992.

Jeffreys, H., and K. E. Bullen, *Seismological Tables*, British Association for the Advancement of Science, Burlington House, London, 1940.

Kendall, J-M., and C. J. Thomson, Seismic modelling of subduction zones with inhomogeneity and anisotropy, I: Teleseismic *P*-wavefront geometry, *Geophys. J. Int.*, *112*, 39-66, 1993.

Knittle, E., and R. Jeanloz, Earth's core-mantle boundary: Results of experiments at high pressure and temperatures, *Science*, *251*, 1438-1443, 1991.

Krüger, F., M. Weber, F. Scherbaum, and J. Schlittenhardt, Double beam analysis of anomalies in the core-mantle boundary region, *Geophys. Res. Lett.*, *20*, 1475-1478, 1993.

Lay, T., Evidence for a lower mantle shear velocity discontinuity in *S* and *sS* phases, *Geophys. Res. Lett.*, *13*, 1493-1496, 1986.

Lay, T., Structure of the core-mantle transition zone: A chemical and thermal boundary layer, *Eos Trans. AGU*, *70*, 54-55, 58-59, 1989.

Lay, T., and D. V. Helmberger, A lower mantle *S*-wave triplication and the shear velocity structure of D'' , *Geophys. R. Astron. Soc.*, *75*, 799-837, 1983.

Masters, T. G., H. F. Bolton, and P. M. Shearer, Large-scale 3-dimensional structure of the mantle, *Eos Trans. AGU*, *73 (14)*, Spring Meeting suppl., 201, 1992.

Nataf, H-C., and S. Houard, Seismic discontinuity at the top of D'': A world-wide feature?, *Geophy. Res. Lett.*, *20*, 2371-2374, 1993.

Phipps Morgan, J., and P. M. Shearer, Seismic constraints on flow and discontinuity topography near 660 km – New evidence for whole mantle convection, *Nature*, *365*, 506-511, 1993.

Revenaugh, J., and T. H. Jordan, Mantle layering from *ScS* reverberations, 4, The lower mantle and core-mantle boundary, *J. Geophys. Res.*, *96*, 19,811-19,824, 1991.

Schlittenhardt, J., J. Schweitzer, and G. Müller, Evidence against a discontinuity at the top of D'', *Geophys. J. R. Astron. Soc.*, *81*, 295-306, 1985.

Shearer, P. M., Imaging global body wave phases by stacking long-period seismograms, *J. Geophys. Res.*, *96*, 20,353-20,364, 1991.

Silver, P. G., R. W. Carlson, and P. Olson, Deep slabs, geochemical heterogeneity, and the large-scale structure of mantle convection: Investigation of an enduring paradox, *Annu. Rev. Earth Planet. Sci.*, *16*, 477-541, 1988.

Stacey, F. D., and D. E. Loper, The thermal boundary layer interpretation of D'' and its role as a plume source, *Phys. Earth Planet. Inter.*, *33*, 45-55, 1983.

Tackley, P. J., D. J. Stevenson, G. A Glatzmaier, and G. Schubert, Effects of an endothermic phase transition at 670 km depth in a spherical model of convection in the Earth's mantle, *Nature*, *361*, 699-704, 1993.

Vidale, J. E., and H. M. Benz, Seismological mapping of fine structure near the base of the Earth's mantle, *Nature*, *361*, 529-532, 1993.

Weber, M., *P*- and *S*-wave reflections from anomalies in the lowermost mantle, *Geophys. J. Int.*, *115*, 183-210, 1993.

Weber, M., and J. P. Davis, Evidence of laterally inhomogeneous lower mantle structure from *P*- and *S*-waves, *Geophys. J. Int.*, *102*, 231-255, 1990.

Weber, M., and M. Körnig, A search for anomalies in the lowermost mantle using seismic bulletins, *Phys. Earth Planet. Inter.*, *73*, 1-28, 1992.

Wessel, P., and W. H. F. Smith, Free software helps map and display data, *Eos Trans. AGU*, *72*, 441, 445-446, 1991.

Wright, C., K. J. Muirhead, and A. E. Dixon, The P wave velocity structure near the base of the mantle, *J. Geophys. Res.*, *90*, 623-634, 1985.

Woodward, R. L., and T. G. Masters, Lower mantle structure from $ScS - S$ differential travel times, *Nature*, *352*, 231-233, 1991.

Woodward, R. L., A. M. Forte, W.-J. Su, and A. M. Dziewonski, Constraints on the large-scale structure of the Earth's mantle, in *Evolution of the Earth and Planets, Geophys. Monogr. Ser.*, *74*, edited by E. Takehashi, R. Jeanloz, and D. Rubie, 89-109, AGU, Washington, D.C., 1993.

Wysession, M. E., E. A. Okal, and C. R. Bina, The structure of the core-mantle boundary from diffracted waves, *J. Geophys. Res.*, *97*, 8749-8764, 1992.

Young, C. J., and T. Lay, Evidence for a shear velocity discontinuity in the lower mantle beneath India and the Indian Ocean, *Phys. Earth Planet. Inter.*, *49*, 37-53, 1987.

Young, C. J., and T. Lay, The core shadow zone boundary and lateral variations of the P velocity structure of the lowermost mantle, *Phys. Earth Planet. Inter.*, *54*, 64-81, 1989.

Young, C. J., and T. Lay, Multiple phase analysis of the shear velocity structure in the D'' region beneath Alaska, *J. Geophys. Res.*, *95*, 17,385-17,402, 1990.

Yuen, D. A., and W. R. Peltier, Mantle plumes and the thermal stability of the D'' layer, *Geophys. Res. Lett.*, *7*, 625-628, 1980.

J-M. Kendall, Department of Physics, 60 St. George Street, University of Toronto, Toronto, ON, M5S 1A7, Canada.

P. M. Shearer, Institute of Geophysics and Planetary Physics, Scripps Institution of Oceanography, University of California, San Diego, La Jolla, CA, 92093.

(Received August 23, 1993; revised December 1, 1993; accepted January 22, 1994.)